Modified Broadside-Coupled Microstrip Lines Suitable for MIC and MMIC Applications and a New Class of Broadside-Coupled Band-Pass Filters

Michael Tran and Cam Nguyen, *Senior Member, IEEE*

Abstract— **Modified broadside-coupled microstrip lines, suitable for microwave and millimeter-wave integrated and monolithic integrated circuit (MIC and MMIC) applications requiring wide bandwidths and tight couplings, are presented. Their analysis, based on the quasi-static spectral domain technique, is described. Using these broadside structures, a new class of broadside-coupled band-pass filters has been developed at X-band (8–12 GHz) with about 1-dB insertion loss. Fair agreement between the measured and calculated results has been observed even though a major approximation is used.**

I. Introduction

THE broadside-coupled structure was first reported by Dalley [1] using the stripline technique. It has an inherent broad-band characteristic, resulting form the strong coupling produced by the two broadside-coupled strips. As pointed out in [2], this structure also has several additional desirable performances and properties not achievable by the edge-coupled counterpart, such as multipole stop-band and multizero pass-band response from a single filter section, due to its large ratios between the even- and odd-mode phase velocities. Variations of the original broadside-coupled stripline have been proposed [2]–[6]. However, a review of the literature reveals that none of the reported structures is suitable for MMIC's and, to some extent, MIC's. For instance, the substrate was assumed to be suspended in air in unsymmetrical broadside structures with strips of equal [5] and unequal widths [6], and identical dielectric layers above and below the upper and lower strips, respectively, in symmetrical versions were employed in [2]–[4]. These structures are stripline-type transmission lines and, clearly, not applicable to MMIC's.

We propose in this paper modified broadside-coupled microstrip lines, as shown in Fig. 1. The proposed transmission lines are applicable to both symmetrical structure, where the two conducting strips are located on top of each other, and unsymmetrical structure, where there is an offset between the strips. Both open [Fig. 1(b)] and shielded [Fig. 1(a)] versions are suitable for MIC applications, while the open structure would be an attractive candidate for MMIC's. The quasi-static spectral domain approach (SDA) [7] is employed to evaluate the capacitances per unit length corresponding to equal and opposite potential excitations, from which the c and π propagating modes are derived. Various numerical results for the mode characteristic impedances and effective dielectric constants of the modified broadside-coupled microstrip lines are presented and discussed. Full-wave analyses for similar structures have been developed [8]–[10]. They, however, only evaluate the reflection and transmission coefficients.

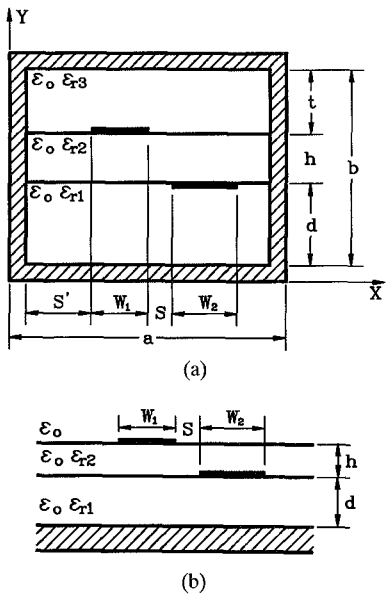

Fig. 1. Cross sections of the modified broadside-coupled microstrip lines: (a) shielded and (b) open.

The microstrip and stripline half-wavelength coupled line band-pass filters [11], [12] have perhaps been the most widely used microwave band-pass filters in the past several decades. Recently, a modified version, with improved stop-band rejection and response symmetry, has also been developed [13]. One shortcoming of this class of filters is the limited bandwidth imposed by a weak coupling between the parallel transmission lines. Various efforts have been made in broadening its operating bandwidth with limited success [14], [15] due to the use of microstrip and stripline that have weak couplings. None of the efforts so far has been reported to realize half-wavelength coupled line band-pass filters using broadside-coupled lines in spite of their inherent broad-band property.

In this paper, we report, for the first time, the development of a new class of half-wavelength coupled line band-pass

Manuscript received May 7, 1992; revised January 26, 1993. This work was supported in part by the NASA Center for Space Power and by TRW Inc.

The authors are with the Electromagnetics and Microwave Laboratory, Department of Electrical Engineering, Texas A&M University, College Station, TX 77843-3128.

IEEE Log Number 9210230.

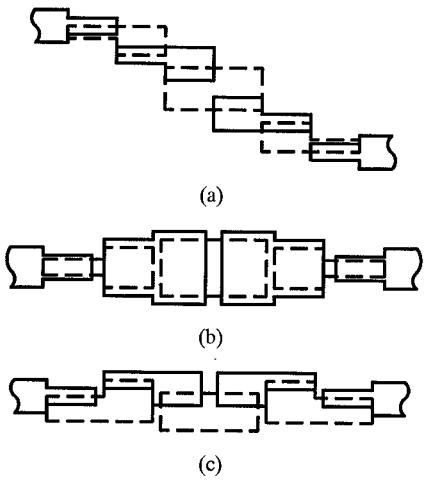

Fig. 2. New broadside-coupled bandpass filters; top (——) and bottom (---).

filters, shown in Fig. 2, employing the proposed broadside-coupled structures. In comparison to the conventional microstrip and stripline coupled line filters, the new filters have wider bandwidths due to the inherently strong coupling achieved between the resonators. Moreover, these filters are very suitable for MIC's as well as MMIC's due to the use of a supported dielectric layer underneath the lower strip. Four three-section band-pass filters have been built and tested in X-band (8–12 GHz) with around 1-dB insertion loss. Reasonably fair agreement between the calculated and experimental performances has also been achieved.

II. Broadside-Coupled Analysis

Fig. 1 shows the cross sections of the shielded and open broadside-coupled microstrip lines which were considered. The structures are assumed to be uniform and infinite in the z-direction. Both the shielded and conducting strips are assumed to be perfectly conducting, and the dielectric substrates are assumed to be lossless. In addition, infinitely thin strips are assumed. Notice that the structures are asymmetric and thus there is no even- or odd-mode existing in the structures. Rather, there are two quasi-TEM propagation modes, referred to as the c-mode and the π-mode corresponding to in-phase and out-of-phase potential excitations, respectively, similar to ones in the two asymmetric parallel coupled lines immersed in an inhomogeneous medium [16]. Here, we only describe the analysis for the shielded structure [Fig. 1(a)]. Results can then be applied to the open version by letting $\varepsilon_{r3} = 1$, and t and a be equal to infinity. Furthermore, results are also applicable to the single suspended substrate stripline or microstrip line by setting the bottom strip width or the bottom dielectric height to zero, respectively. We first utilize the quasi-static SDA [7] to determine the per-unit-length capacitances corresponding to equal and opposite potential excitations. Finally, we evaluate the c- and π-mode capacitances per unit length and then the corresponding mode characteristic impedances and effective dielectric constants. One remark appropriate here is that, although there exist two c- and two π-mode characteristic impedances for the considered coupled structures, one can choose their dimensions, W_1, W_2, S, and S' (for a shielded structure), to produce equal c-mode impedances and equal π-mode impedances. This fact is exploited in the filter design to be discussed later.

A. Formulation

Detailed quasi-static SDA was presented in [7], so here we only describe the essential steps. By imposing the boundary conditions at the interfaces along the y-direction in the spectral domain, obtained as the Fourier transforms of those in the space domain, and applying Galerkin's method along with Parseval's theorem, we can derive the following system of linear equations:

$$\sum_{k=1}^{K} K_{ik}^{11}\left(\hat{k}_n\right) a_k + \sum_{m=1}^{M} K_{im}^{12}\left(\hat{k}_n\right) b_m = P_i, \quad i = 1, 2, \cdots, K \tag{1a}$$

$$\sum_{k=1}^{K} K_{jk}^{21}\left(\hat{k}_n\right) a_k + \sum_{m=1}^{M} K_{jm}^{22}\left(\hat{k}_n\right) b_m = Q_i, \quad j = 1, 2, \cdots, M \tag{1b}$$

where

$$K_{ik}^{11}\left(\hat{k}_n\right) = \sum_{n=1}^{\infty} \tilde{\rho}_{1i}\left(\hat{k}_n\right) \tilde{G}_{11}\left(\hat{k}_n\right) \tilde{\rho}_{1k}\left(\hat{k}_n\right) \tag{2a}$$

$$K_{im}^{12}\left(\hat{k}_n\right) = \sum_{n=1}^{\infty} \tilde{\rho}_{1i}\left(\hat{k}_n\right) \tilde{G}_{12}\left(\hat{k}_n\right) \tilde{\rho}_{2m}\left(\hat{k}_n\right) \tag{2b}$$

$$K_{jk}^{21}\left(\hat{k}_n\right) = \sum_{n=1}^{\infty} \tilde{\rho}_{2j}\left(\hat{k}_n\right) \tilde{G}_{21}\left(\hat{k}_n\right) \tilde{\rho}_{1k}\left(\hat{k}_n\right) \tag{2c}$$

$$K_{jk}^{21}\left(\hat{k}_n\right) = \sum_{n=1}^{\infty} \tilde{\rho}_{2j}\left(\hat{k}_n\right) \tilde{G}_{21}\left(\hat{k}_n\right) \tilde{\rho}_{1k}\left(\hat{k}_n\right) \tag{2d}$$

$$\tilde{G}_{11} = \frac{1}{\Delta}\left(\varepsilon_{r1} + \varepsilon_{r2} \coth \hat{k}_n h \cdot \tanh \hat{k}_n d\right) \tag{3a}$$

$$\tilde{G}_{12} = \tilde{G}_{21} = \frac{1}{\Delta}\varepsilon_{r2}\left(\frac{\tanh \hat{k}_n d}{\tanh \hat{k}_n h}\right) \tag{3b}$$

$$\tilde{G}_{12} = \frac{1}{\Delta}\left(\varepsilon_{r3} \coth \hat{k}_n t + \varepsilon_{r2} \coth \hat{k}_n h\right) \tanh \hat{k}_n d \tag{3c}$$

$$\Delta = \varepsilon_0 \left[\varepsilon_{r3} \coth \hat{k}_n t \left(\varepsilon_{r1} + \varepsilon_{r2} \coth \hat{k}_n h \cdot \tanh \hat{k}_n d\right) + \varepsilon_{r2}\left(\varepsilon_{r2} \tanh \hat{k}_n d + \varepsilon_{r1} \coth \hat{k}_n h\right)\right] \tag{4a}$$

$$\hat{k}_n = \frac{n\pi}{a} \tag{4b}$$

$$P_i = \frac{2}{a} V_1 \int_0^a \rho_{1i}(x)\, dx \tag{5a}$$

$$Q_j = \frac{2}{a} V_2 \int_0^a \rho_{2j}(x)\, dx \tag{5b}$$

with ρ_{1i} and ρ_{2j} being the known basis functions that, together with the unknown constants a_i and b_j, describe the respective charge distributions on the upper and lower strips. The tilde ($\tilde{}$) indicates the Fourier-transformed quantity. V_s, $s = 1, 2$, denote the known potentials on the upper strip ($s = 1$) and lower strip ($s = 2$).

The above equations can be applied to the open structure [Fig. 1(b)] by setting ε_{r3} to 1, and t and a infinity.

Now, by exciting the upper and lower strips with equal $(V_1 = V_2 = 1)$ and opposite $(V_1 = -V_2 = 1)$ potentials, we can obtain the corresponding quasi-static capacitances per unit length, $C_{(e),s}$ and $C_{(o),s}$, $s = 1, 2$, for the strips as follows:

$$C_{(e \text{ or } o),1} = \frac{a}{2V_1^2} \sum_{k=1}^{K} a_k P_k \tag{6a}$$

$$C_{(e \text{ or } o),2} = \frac{a}{2V_2^2} \sum_{k=1}^{K} b_m Q_m \,. \tag{6b}$$

The quasi-static per-unit-length capacitances $C_{p,s}$ of the strips for mode p, $p = c, \pi$, can then be computed from [17]

$$C_{p,1} = C_{(e),1} + 0.5\big(C_{(o),1} - C_{(e),1}\big)\big(1 - R_p\big) \tag{7a}$$

$$C_{p,2} = C_{(e),2} + 0.5\big(C_{(o),2} - C_{(e),2}\big)\big(1 - R_p^{-1}\big) \tag{7b}$$

where $R_{c,\pi}$ are the ratios of the voltages on the strips for modes c and π, and can be evaluated from the even- and odd-excitation capacitances per unit length of the strips [17]. Once $C_{p,s}$ are found, c- and π-mode characteristic impedances, effective dielectric constants, and phase velocities can be determined.

B. Numerical Results

To obtain numerical results, we have employed Chebyshev polynomials of the first kind, along with the Maxwellian terms, for the basis functions [5], [6]. These functions describe closely the charge distributions on the strips due to the inclusion of the edge effect.

To verify the developed analysis, numerical results are compared to [3] and [5]. Fig. 3 compares calculated results of the even- and odd-mode characteristic impedances to those reported in [3, Fig. 14] for an enclosed symmetrical structure. In Fig. 4, a comparison between the computed mode characteristic impedances and those in [5, Fig. 2] for a structure having a form of odd symmetry is made. As a result, the c-mode impedances are the same for both lines and can be called Z_{oe}. Similarly, the π-mode impedances are the same and can be called Z_{oo}. It can be seen that our calculated results match very well to the existing data.

Fig. 5 shows variations of the c- and π-mode characteristic impedances and effective dielectric constants versus the lower strip width for a shielded structure. The strips centers are aligned at the center of the shield, and the middle substrate has $\varepsilon_{r2} = 2.2$ and the others have $\varepsilon_{r1} = 1$ and $\varepsilon_{r3} = 1$. One can see that as the lower strip width is increased, the mode characteristic impedances corresponding to the lower strip decrease, while those corresponding to the upper strip increase and remain virtually the same for the c- and π-mode, respectively.

Calculated values of the mode characteristic impedances and effective dielectric constants of an open structure are plotted as a function of the distance between the strip edges as shown in Fig. 6. The relative dielectric constants are $\varepsilon_{r1} = 2.2$, $\varepsilon_{r2} = 10.5$, and $\varepsilon_{r3} = 1$. The c- and π-mode characteristic

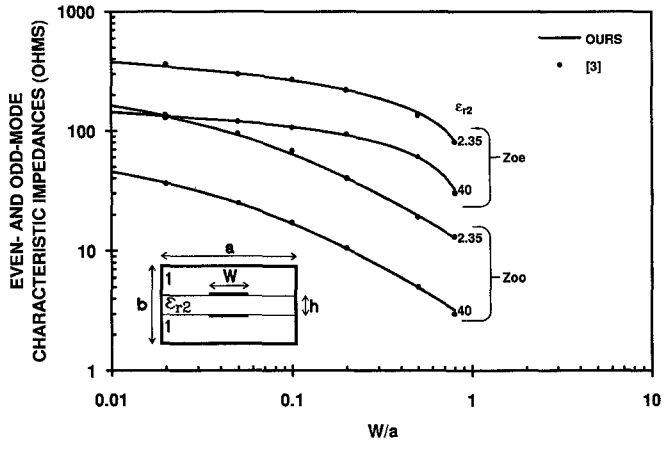

Fig. 3. Even- and odd-mode characteristic impedances versus W/a for a symmetric structure enclosed in metal. Z_{oe} and Z_{oo} are even- and odd-mode characteristic impedances, respectively $(b/a = 4,\ h/a = 0.1)$.

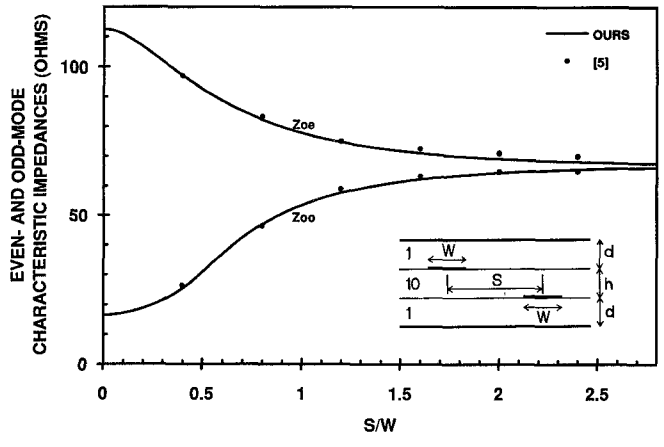

Fig. 4. Even- and odd-mode characteristic impedances for an offset structure with equal strip widths as a function of S/W. $(0.5 + d)/W = 1$, $0.5/W = 0.2$. Note that the structure still has symmetry.

impedances decrease and increase, respectively, as the distance is increased. The trend of the curves shows that as the distance between the strips is very large, the c- and π-mode characteristic impedances should become equal for a given strip, since no coupling will occur, and hence the upper and lower lines are isolated. The π-mode effective dielectric constant for strip 1 or 2 decreases significantly, whereas that of the c-mode is virtually unchanged with increase in the strips' distance.

III. Filter Design and Performance

New half-wavelength coupled line band-pass filters, employing the broadside-coupled microstrip lines, are shown in Fig. 2. The filter design is based upon [12]. From given band-pass filter specifications, a low-pass to band-pass transformation is used to determine the number of resonators required. The low-pass prototype filter's element values are then obtained, and the even- and odd-mode characteristic impedances of the corresponding band-pass filter are computed. These even- and odd-mode impedances correspond to our c- and π-mode impedances, respectively. There are two even- and two odd-mode impedances for each coupled section located at

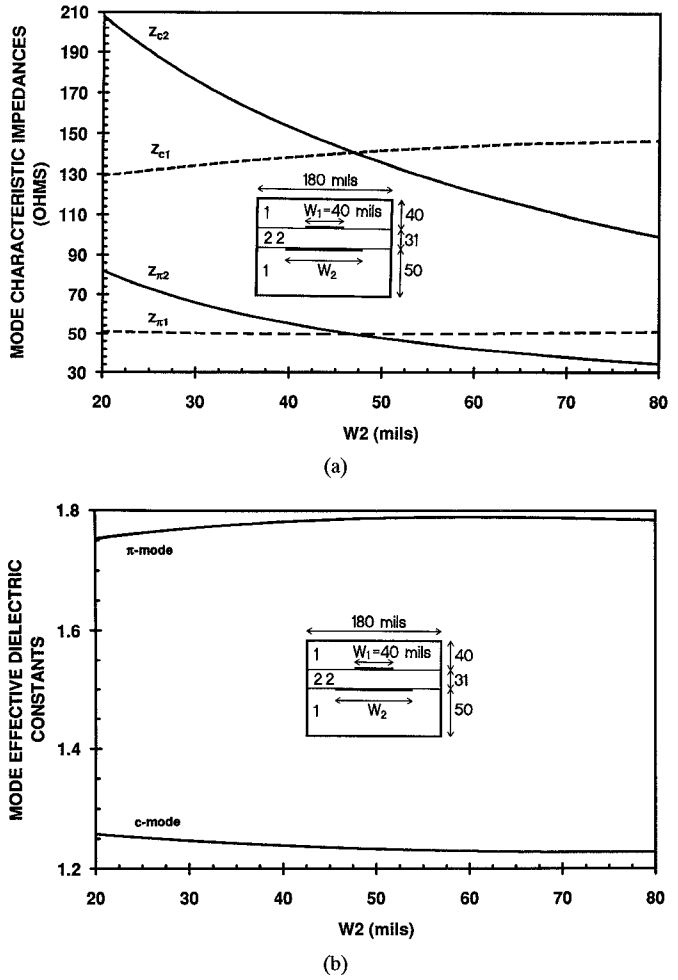

Fig. 5. c- and π-mode characteristic impedances (a) and effective dielectric constants (b) as a function of W_2 with W_1 constant. Z_{ps}, $p = c, \pi$ and $s = 1, 2$, are mode characteristic impedances.

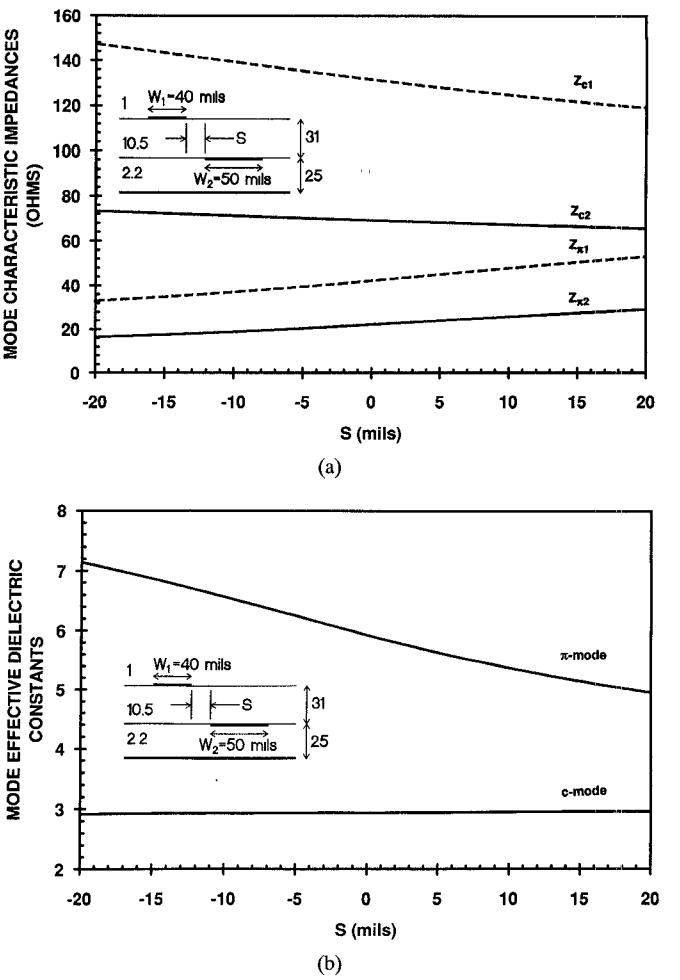

Fig. 6. c- and π-mode characteristic impedances (a) and effective dielectric constants (b) as a function of S.

both ends, resulting from the filter synthesis [12]. The widths of the broadside-coupled strips W_1 and W_2, the distance between the strip edges S, and the spacing between the channel wall and the first strip edge S' (for a shielded structure) are chosen to correspond to these synthesized even- and odd-mode impedances. For the interior coupled sections, however, only one even-mode and one odd-mode impedance are obtained for each section, according to [12]. The dimensions of the interior broadside-coupled strips, W_1, W_2, S, and S', are thus chosen so that there exists equal c-mode and equal π-mode impedances, whose values are the same as those of the synthesized even- and odd-mode impedances, respectively; i.e., there are only one c- and one π-mode impedance in each of the filter interior coupled-line sections. Next, the average of the c- and π-mode phase velocities is used in determining the length of each coupled section, as commonly done for filters employing inhomogeneous media such as microstrip coupled-line filters. Finally, the filter response is calculated by using an equivalent-circuit model of the inhomogeneous coupled-line section [16] that takes into account the different c- and π-mode velocities. Note that the use of an average velocity to obtain the lengths of coupled-line sections ignores the forward coupling due to the sizable velocity differences, which can cause an undesired filter response. This problem, however, can be solved by using an optimization routine to modify the design so as to obtain the desired performance.

Four different filters—one enclosed structure and three open structures—were designed and tested. All filters have 0.1-dB pass-band ripple, three sections, and center frequencies of 10 GHz. The open filter structures, whose physical layouts are shown in Fig. 2, are of microstrip type having ground planes only at the bottom, as illustrated in Fig. 1(b). Fig. 2(a), with equal or unequal strip widths, has the same basic layout as that of the conventional half-wavelength coupled line filter [1], [12], whereas in Fig. 2(b), the strips are located directly on top of each other about the centerline but with different widths. The layout in Fig. 2(c) employs an asymmetrical broadside structure with an offset between the upper and lower strips. These filters were fabricated on Duroid substrates with $\varepsilon_{r1} = 2.2$ and $h_1 = 31$ mil, $\varepsilon_{r2} = 10.5$ and $h_2 = 25$ mil, and $\varepsilon_{r3} = 1.0$. The enclosed filter structure [see Fig. 1(a)] has the same basic layout as in Fig. 2(c). It is of suspended substrate stripline type with air on the top and bottom regions and enclosure dimensions of $a = 180$ mil and $b = 131$ mil. It was realized on a Duroid substrate with a relative dielectric constant of 2.2 and a thickness of 31 mil.

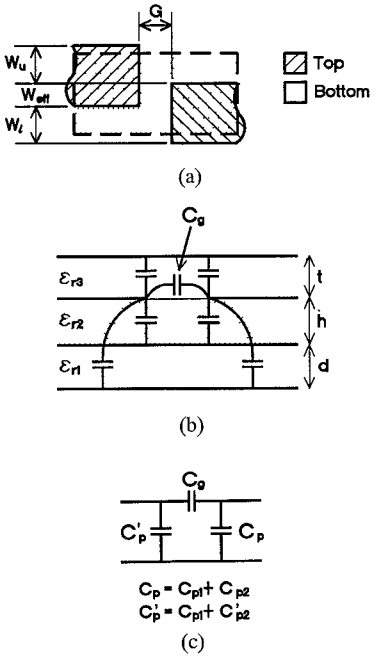

Fig. 7. Top view (a) and side view (b) of an actual gap and its equivalent circuit (c).

In order to calculate the filter responses, equivalent circuits for the gaps and open ends [see Fig. 7(a)], encountered in the filters (Fig. 2), need to be determined. Consider an actual gap layout along with its equivalent circuit, as shown in Fig. 7, that consists of an asymmetric (offset) gap on one side of the substrate and a continuous transmission line on the other side. The gap capacitances for the symmetric gap of line width W_{eff} and gap width G resemble those of a microstrip gap configuration having a dielectric thickness of h. This enables us to approximate C_g and C_{p1} as [18]

$$C_g = W_{eff}(C_{fo} - C_{fe}) \tag{8a}$$

$$C_{p1} = W_{eff}C_{fe} \tag{8b}$$

where C_{fe} and C_{fo} are the respective even- and odd-symmetric fringing capacitances per unit length. C_{p2} and C'_{p2} may be approximately calculated as

$$C_{p2} = W_u C_f \tag{9a}$$

$$C'_{p2} = W_l C_f \tag{9b}$$

where C_f represents the fringing capacitance to ground. The open-end capacitance is obtained by using a large value for G.

Fig. 8 shows the experimental and theoretical results of the enclosed filter structure [Fig. 2(c)]. As can be seen, they match almost exactly. Figs. 9–11 are the performances of the open structures. Notice that the agreement between the measured and calculated results for the open structures [Fig. 2(c)] is not as good as that of the enclosed structure. A downward frequency shift of about 10% from the calculated performance has occurred. Nevertheless, it is reasonably good considering the approximations we have used in calculating the gap capacitances. More accurate analysis for the gaps and open ends (Fig. 7) needs to be derived and used in the filter design. But this is beyond the scope of this work. All filters exhibit

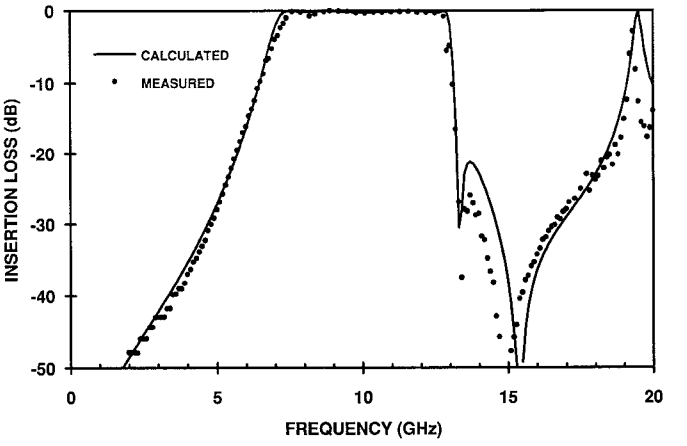

Fig. 8. Performance of the enclosed broadside-coupled bandpass filter as shown in Fig. 2(c). The cross section was as shown in Fig. 1(a) with $\varepsilon_{r1} = \varepsilon_{r3} = 1$, $\varepsilon_{r2} = 2.2$, $d = t = 50$ mils, $h = 31$ mils, and $a = 180$ mils.

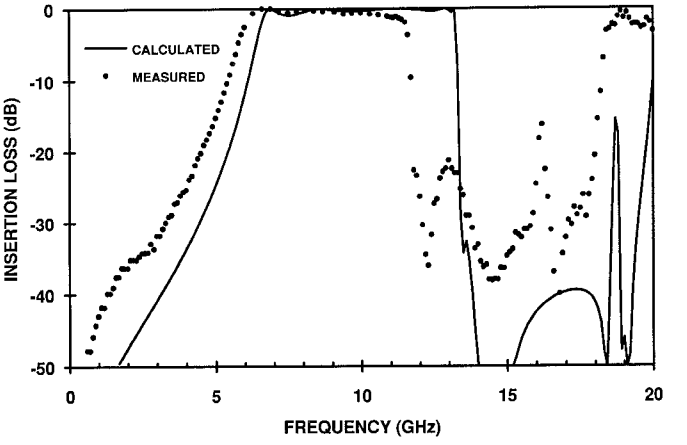

Fig. 9. Performance of the open broadside-coupled bandpass filter as shown in Fig. 2(c). The cross section was as shown in Fig. 1(b) with $\varepsilon_{r1} = 2.2$, $\varepsilon_{r2} = 10.5$, $\varepsilon_{r3} = 1$, $d = 25$ mils, $h = 31$ mils.

pass-band insertion losses of about 1 dB. It is also apparent from Figs. 8–12 that the filters with gaps between resonator ends on the same substrate sides [Fig. 2(b), (c)] possess wider stop-bands with higher rejection near the upper stop-band edge than that of the conventional layout filter (Fig. 2(a)]. This is due to the fact that the former filters have additional poles of attenuation produced by the extra couplings at the end gaps. Furthermore, the filters in Fig. 2(b), (c) occupy significantly less space than that of Fig. 2(a), and thus are very attractive for applications requiring small circuit sizes or in MMIC's where GaAs real estate is too expensive. Photographs of the enclosed filter and one open filter are given in Figs. 12 and 13, respectively.

IV. Conclusions

Modified broadside-coupled microstrip lines, suitable for broad-band and tight-coupling MIC and MMIC applications, have been proposed. The proposed transmission lines are applicable to both symmetrical and asymmetrical structures. Analysis of mode characteristics, based on the quasi-static

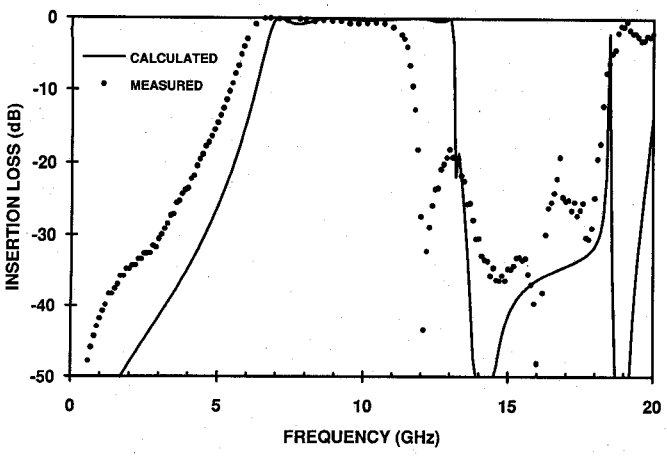

Fig. 10. Performance of the open broadside-coupled bandpass filter as shown in Fig. 2(b). The cross sections was as shown in Fig. 1(b) with $\varepsilon_{r1} = 2.2$, $\varepsilon_{r2} = 10.5$, $\varepsilon_{r3} = 1$, $d = 25$ mils, $h = 31$ mils.

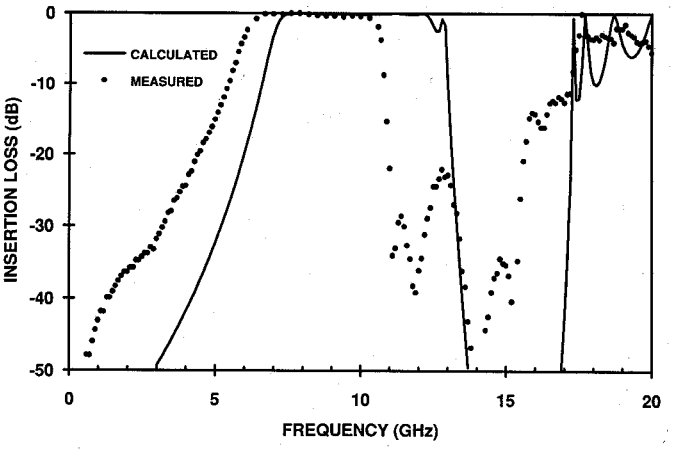

Fig. 11. Performance of the open broadside-coupled bandpass filter as shown in Fig. 2(a). The cross section was as shown in Fig. 1(b) with $\varepsilon_{r1} = 2.2$, $\varepsilon_{r2} = 10.5$, $\varepsilon_{r3} = 1$, $d = 25$ mils, $h = 31$ mils.

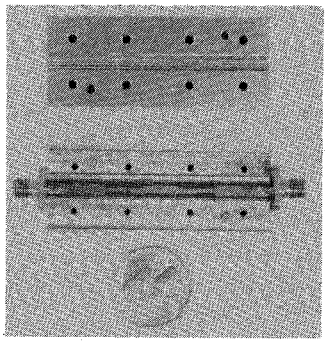

Fig. 12. Photograph of the enclosed broadside-coupled bandpass filter.

SDA, has also been presented along with numerical results of the mode characteristic impedances and effective dielectric constants. Various new half-wavelength broadside-coupled band-pass filters have been developed. Measured performances of fabricated three-resonator filters at 10 GHZ are in fair agreement with the predicted results. In particular, the new filters with gaps alternate between resonators, besides taking much less space, possess wider stop-band than that without the gaps. The reported transmission lines and filter structures

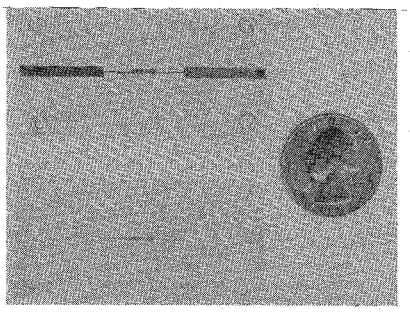

Fig. 13. Photograph of an open broadside-coupled bandpass filter (top and bottom sides).

should be very useful for MIC's as well as MMIC's, because they show a great capability for achieving broad bandwidths and tight couplings.

ACKNOWLEDGMENT

The authors wish to thank L. Fan for his technical support. They would also like to thank the anonymous reviewers for many useful comments and suggestions.

REFERENCES

[1] J. E. Dalley, "A strip-line directional coupler utilizing a non-homogeneous dielectric medium," *IEEE Trans. Microwave Theory Tech.*, vol. MTT-17, pp. 706–712, Sept. 1969.
[2] J. L. Allen, "Inhomogeneous coupled-line filters with large mode-velocity ratios," *IEEE Trans. Microwave Theory Tech.*, vol. MTT-22, pp. 1182–1186, Dec. 1974.
[3] J. L. Allen and M. F. Estes, "Broadside-coupled strips in a layered dielectric medium," *IEEE Trans. Microwave Theory Tech.*, vol. MTT-20, pp. 662–669, Oct. 1972.
[4] I. J. Bahl, "Characteristics of inhomogeneous broadside-coupled striplines," *IEEE Trans. Microwave Theory Tech.*, vol. MTT-28, pp. 529–535, June 1980.
[5] T. Kitazawa *et al.*, "Unsymmetric broadside-coupled striplines," *Electron. Lett.*, vol. 18, pp. 425–426, May 1982.
[6] T. Kitazawa and Y. Hayashi, "Analysis of unsymmetrical broadside-coupled striplines with anisotropic substrates," *IEEE Trans. Microwave Theory Tech.*, vol. MTT-34, pp. 188–191, Jan. 1986.
[7] T. Itoh and A. S. Hebert, "A generalized spectral domain analysis for coupled suspended microstriplines with tuning septums," *IEEE Trans. Microwave Theory Tech.*, vol. MTT-26, pp. 820–826, Oct. 1978.
[8] H. Y. Yang and N. G. Alexopoulos, "Basic blocks for high-frequency interconnects: Theory and experiment," *IEEE Trans. Microwave Theory Tech.*, vol. MTT-36, pp. 1258–1264, Aug. 1988.
[9] T. S. Horng, H. Y. Yang, and N. G. Alexopoulos, "A full-wave analysis of shielded microstrip line-to-line transitions," in *1990 IEEE MTT-S Int. Symp. Dig.*, pp. 251–254.
[10] W. Schwab and W. Menzel, "On the design of planar microwave components using multilayer structures," *IEEE Trans. Microwave Theory Tech.*, vol. MTT-40, pp. 67–71, Jan. 1992.
[11] S. B. Cohn, "Parallel-coupled transmission line resonator filters," *IRE Trans. Microwave Theory Tech.*, vol. MTT-6, pp. 223–231, Apr. 1958.
[12] G. L. Matthaei, L. Young, and E. M. T. Jones, *Microwave Filters, Impedance-Matching Networks, and Coupling Structures.* New York: McGraw-Hill, 1980.
[13] C. Chang and T. Itoh, "A modified parallel-coupled filter structure that improves the upper stopband rejection and response symmetry," *IEEE Trans. Microwave Theory Tech.*, vol. MTT-39, pp. 310–314, Feb. 1991.
[14] J. A. Mosko, "Design technique for UHF stirpline filters," NAVWEPS Rep. 8677, 1965.
[15] D. Rubin and A. R. Hislop, "Millimeter-wave coupled line filters: Design techniques for suspended structure and microstrip," *Microwave J.*, vol. 23, pp. 67–78, Oct. 1980.
[16] V. K. Tripathi, "Asymmetric coupled transmission line in an inhomogeneous medium," *IEEE Trans. Microwave Theory Tech.*, vol. MTT-23, pp. 734–739, Sept. 1975.

[17] C. Nguyen, "Broadside-coupled coplanar waveguides and their end-coupled band-pass filter applications," *IEEE Trans. Microwave Theory Tech.*, vol. MTT-40, pp. 2181–2189, Dec. 1992.
[18] C. Nguyen and K. Chang, "Design and performance of millimeter-wave end-coupled bandpass filters," *Int. J. Infrared Millimeter Waves*, vol. 6, pp. 497–509, Aug. 1985.

Michael Tran was born in Vietnam, in September 1967. He received the B.S. degree in electrical engineering form Texas A&M University in December 1990.

He is currently pursuing the M.S. degree at Texas A&M. His interest is in microwave and millimeter-wave integrated circuits.

Mr. Tran is a member of Tau Beta Pi.

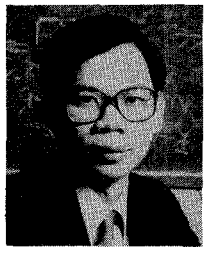

Cam Nguyen received the B.S. degree in Mathematics from the National University of Saigon, Vietnam, and the B.S., M.S., and Ph.D. degrees in Electrical Engineering from the California Polytechnic University, Pomona, the California State University, Northridge, and the University of Central Florida, respectively.

From 1979 to 1982, he was employed by ITT Gilfillan, Van Nuys, CA, where he designed and developed various microwave components for ground- and ship-based radars including power dividers and combiners, filters, frequency doublers and triplers, phase shifters, switches, and power amplifiers. In 1982, he joined Hughes Aircraft Co. in Torrance, CA as a Member of Technical Staff and worked on many millimeter-wave components, from 26.5 to 150 GHz, including mixers, switches, and filters. From 1983 to 1986, he was the TRW, Redondo Beach, CA, where he was responsible for the design and development of advanced millimeter-wave integrated-circuit components, from 26.5 to 170 GHz, including finline and crossbar mixers, subharmonic mixers, multiplexers, filters, oscillators, frequency multipliers, phase shifters, amplifiers, and switches. He also developed various computer programs for the analysis and design of microwave and millimeter-wave integrated circuits. From 1986 to 1987, he was with Aerojet ElectroSystems Co., Azusa, CA, where he was responsible for the design and development of extremely low noise, space-qualified mixers from 60 to 110 GHz for radiometry applications. In 1987, he joined the monolithic group of Martin Marietta Co., Orlando, FL. There he was responsible for the design and development of millimeter-wave monolithic circuits. He was also involved with the development of microstrip and CPW discontinuity models and nonlinear models for MESFETs and HEMTs. In 1989 he returned to the Communication Laboratory of TRW, Redondo Beach, CA as a Senior Staff Engineer, where he was responsible for the development of advanced microwave and millimeter-wave components and subsystems, such as high dynamic range MMIC mixers and multi-channel switched filters, etc. In 1991, he joined the faculty of the Department of Electrical Engineering of the Texas A&M University.

He has published over 55 papers and two book chapters and is listed in *Who's Who in America, Who's Who of Emerging Leaders in America, Who's Who in the West,* and the *International Directory of Distinguished Leadership.* His current research interests encompass both the areas of electromagnetics and microwave electronics with concentrations in the microwave and millimeter-wave circuits, devices, planar transmission lines, receivers, and transmitters.